sustainability

MDPI

Article

Augmented Statistics for Hydroclimatic Extremes: Spearman, Mann–Kendall, and AI Classification for Drought Risk Mapping

Emanuela Genovese [1,2], Clemente Maesano [1] and Vincenzo Barrile [2,*]

[1] Department of Civil, Building and Environmental Engineering (DICEA), Sapienza University of Rome, Via Eudossiana, 18, 00184 Rome, Italy
[2] Department Of Civil Engineering, Energy, Environment and Materials (DICEAM), Mediterranea University of Reggio Calabria, Via Zehender, 89124 Reggio Calabria, Italy
* Correspondence: vincenzo.barrile@unirc.it

Abstract

The effects of climate change are now evident on all scales, both global and local. Extreme events linked to climate change, such as heat islands and water bombs, are occurring with increasing frequency, causing significant harm to humans. Furthermore, rising temperatures also cause significant drought and desertification, which must be carefully assessed and analyzed. For this reason, with a view to evaluating environmentally sustainable development, the following research focuses on the variables that contribute to the reduction in local water availability in the province of Reggio Calabria, considering air temperature, evapotranspiration, precipitation, and available water resources. The Mann–Kendall test revealed a statistically significant increasing trend in air temperature ($Z = +2.5$, $p < 0.01$) and a decreasing tendency in precipitation, while the NDWI analysis indicated a reduction of about 34% in surface water resources between 2019 and 2023. The Spearman test showed strong negative correlations between temperature and water availability ($\rho = -0.68$) and between evapotranspiration and water availability ($\rho = -0.66$). Lastly, four artificial intelligence (AI) classifiers were compared: Random Forest, XGBoost, Gradient Boosting Decision Tree, and Logistic Regression. Random Forest performed the best, with 93% accuracy and 90% precision. The results confirm the strong negative dependence of temperature and evapotranspiration on water resources and identify Random Forest as the most reliable model for determining the area's most at risk of drought.

Keywords: remote sensing; augmented statistics; statistics; climate change; drought

check for updates

Academic Editor: Congzheng Han

Received: 27 September 2025
Revised: 14 October 2025
Accepted: 16 October 2025
Published: 18 October 2025

Citation: Genovese, E.; Maesano, C.; Barrile, V. Augmented Statistics for Hydroclimatic Extremes: Spearman, Mann–Kendall, and AI Classification for Drought Risk Mapping. *Sustainability* **2025**, *17*, 9251. https://doi.org/10.3390/su17209251

Copyright: © 2025 by the authors. Licensee MDPI, Basel, Switzerland. This article is an open access article distributed under the terms and conditions of the Creative Commons Attribution (CC BY) license (https://creativecommons.org/licenses/by/4.0/).

1. Introduction

The drought risk is relentless in Italy, especially in Calabria [1]. Among the cities that are facing the worst critical issues in Italy is Reggio Calabria, where the Aspromonte Forest and the important Menta Dam are located, the latter providing a good part of municipal water needs. Calabria, a Mediterranean region which has always had an abundance of water and lush vegetation, has been suffering from the effects of climate change in recent years, bringing the availability of water in the Calabrian municipalities to increasingly worrying and critical levels. In particular, the factors that trigger these critical conditions are the lack of precipitation, which has the task of raising the level of surface and deep water, and the increasingly less frequent snowfall at high altitudes. However, there are some factors that contribute more significantly to the scarcity of water resources in Calabria and should not be overlooked. In fact, evaporation phenomena cause water reserves

to decrease exponentially. In Italy, as is known, ISPRA (Italian National Institute for Environmental Protection and Research) provides an overview of water severity at a national scale using Permanent District Observatories for water uses. As reported by ISPRA, using the BIGBANG national hydrological balance model, "in the thirty-year period 1991–2020 there was a reduction in the annual average of about 20% (−108.1 mm) compared to an estimate made by the National Water Conference". In the report, it is highlighted that 2022 was the year with the historical minimum of water resources, with a reduction of 50% compared to the annual average of the last thirty years. In 2023, there was also a reduction in the availability of water resources of 18.4% compared to the long-term average. They stated that this is caused by the deficit in precipitation, but also by the increase in water volume of evapotranspiration. ISPRA it-self conducted a study to determine the percentage of Italian territory affected by drought and the state of the watercourses present in the territory, which, regarding the latter, for the Calabria region is currently unknown [2]. To address these drought issues at the international level, United Nations member states have undertaken measures through the 2030 Agenda to mitigate the effects of climate change, setting 17 goals related to specific themes, including drought and desertification, corresponding to Goal 15, which aims to "Protect, restore, and promote the sustainable use of terrestrial ecosystems, sustain-ably manage forests, combat desertification, halt and reverse land degradation, and halt biodiversity loss" [3].

The study of the correlations between climate variables and water scarcity and, consequently, widespread drought phenomena is relevant in scientific literature, together with the possible methods needed to identify the area's most at risk. Some studies, in particular, explore the use of remote sensing and therefore satellite images to map water resources [4] and to determine and correlate geospatial variables from a spatial and temporal point of view [5], in order to identify specifically and on a large scale the points in which the effects of the ever-increasing temperature of the Earth's surface are most felt. The combination of geospatial information deriving from remote sensing can certainly lead to a deeper knowledge of the phenomena that trigger continuous drought periods [6] and therefore allow us to monitor developments and study possible mitigation interventions at a local level.

Numerous studies have investigated the relationship between climate variables; the literature widely documents that an increase in temperatures, associated with higher potential and actual evapotranspiration, leads to a reduction in available water reserves in soils and surface water bodies, especially in Mediterranean climates characterized by strong seasonality. At the same time, interannual variability in precipitation directly affects groundwater recharge and river flow, accentuating periods of water deficit in the warmer months. Analyzing the correlations between these variables is therefore a consolidated and fundamental approach to understanding drought processes. About it, Němec and Schaake [7] address the problem of how water systems respond to climate variations by trying to focus on the evaluation of their sensitivity even to moderate climate variations and extreme events. This is done using deterministic models, studying how the flow of rivers varies and their behavior in extreme conditions, concluding that climate variations, even those they define as "moderate", can have a decidedly significant impact on water resources. Xu et al. [8] also study how climate change has affected temperature, precipitation and runoff using climate time series and parametric and non-parametric techniques, highlighting in their results that temperature has steadily increased in recent years. Moses and Hambira [9] address the problem of water loss through evapotranspiration, analyzing climate trends to understand how climate change is acting by modifying these natural dynamics. The study was conducted using wind speed, solar radiation and relative humidity and the Mann–Kendall test to analyze the trends of the collected climate data, concluding that the increase in the aforementioned climate parameters will tend to increase evapotran-

spiration and therefore the water loss due to this condition. An important scientific review on evapotranspiration [10] highlights a significant increase in this variable on a global scale, with marked interdecadal variability. The main causes identified for this increase are vegetation greening (increase in the Leaf Area Index), increased atmospheric evaporative demand, and increased precipitation. The analysis is not limited to the global scale, but also delves into regional trends, showing how, in temperate zones, a particularly significant increase in evapotranspiration is recorded.

The identification of areas most at risk of drought, therefore, is of great importance and utility and is strongly linked to the aforementioned climatic factors. To this end, several techniques exist that can provide a valuable contribution, the most innovative of which concern the use of advanced geomatics methodologies, in particular remote sensing and artificial intelligence algorithms [11,12]. The latter, applied to geospatial data, can provide detailed and highly valuable information on the environmental and territorial conditions of the areas under study. Classification algorithms, as is known, can be divided into supervised and unsupervised, each of which presents specific advantages in relation to different contexts and different applications [13–15]. Lima et al. [16], for example, present a method to classify drought using four indices in order to characterize the frequency and severity of drought in a particular river in Brazil, mainly using 89 rainfall stations and the Thiessen polygon method to calculate the mean precipitation, highlighting that the river taken as a case study in recent years is experiencing a severe climatic drought.

It is evident that a more in-depth knowledge of these dynamics, at a detailed level, and a accurate instrument to detect the area's most at risk, allows individual communities to make specific decisions for their territory, and the possibility of using a cloud-based solution guarantees speed of execution and a high level of information.

In this context, the problem addressed in this work is the limited availability of spatially continuous and locally validated information for the estimation of water availability and the characterization of drought risk in the province of Reggio Calabria. Although previous studies have investigated these phenomena, the present research is distinguished by the combined use of remote sensing data and artificial intelligence algorithms, which allows for a more detailed and operational assessment of hydro-climatic dynamics at the local scale. The main objectives are: (1) to quantify the spatio-temporal trends of the main climatic factors (temperature, precipitation, evapotranspiration) and surface water cover using satellite products (Sentinel, MODIS, Global Precipitation Measurement) on the Google Earth Engine (GEE) platform; (2) to evaluate the spatio-temporal correlations between these factors and water availability using a non-parametric tests (Mann–Kendall, Spearman); (3) to develop and compare classification models based on ensemble algorithms (Random Forest, XGBoost, Gradient Boosting Decision Tree, Logistic Regression) to map areas at desertification risk at the municipal scale. The results aim to provide a replicable and operation-ready tool to support local decisions on water resources management and land use planning. The study combines augmented statistics and artificial intelligence to address the problem related to the effects of climate change. The novel aspect of the paper is not just the validation of the inverse relationship between climate factors and water resources, but additionally the combination of artificial intelligence techniques and remote sensing data applied to a particular region of the Mediterranean. Therefore, the main goals were to describe the hydroclimatic interactions in this particular local context, determine which satellite indices were most important, and choose the best classification system. Although it was created for a small case study, this method is meant to be applied to various regions by adjusting to the local indicators that are available.

2. Study Area

The study area chosen to apply the methodology outlined above is the entire province of Reggio Calabria (Figure 1), which includes part of the Aspromonte National Park. The Aspromonte National Park is one of Calabria's most important protected areas, rich in biodiversity and natural, historical, and cultural significance. The Park is a UNESCO Geopark and is home to 1500 species of flora and an extraordinary wealth of fauna, covering a total area of 1965 km^2. The Geopark is divided into thematic areas: the Piana di Gioia area, the Strait area, the Grecanic area, and the Locride area, as well as the heart of the Park, which includes the Menta Dam. This dam is one of Calabria's main water infrastructures and has a capacity to retain approximately 20 million cubic meters of water, a significant reserve for the water supply of several Calabrian municipalities, including Reggio Calabria. Calabria is also characterized by the presence of water bodies typical of the Mediterranean and southern Italy, "fiumare", which are known to have the characteristic of having a short course, characterized by a long bed, and a water flow that is generally higher during the autumn and winter periods. The study, then, focuses on a specific portion of the National Geopark located in the Locride area, which, due to its unique conformation, was chosen as the area for the classification of areas potentially at risk of drought. Indeed, despite the vegetation present in the territory, the area is often characterized by severe drought periods that cause significant damage to crops in agricultural areas.

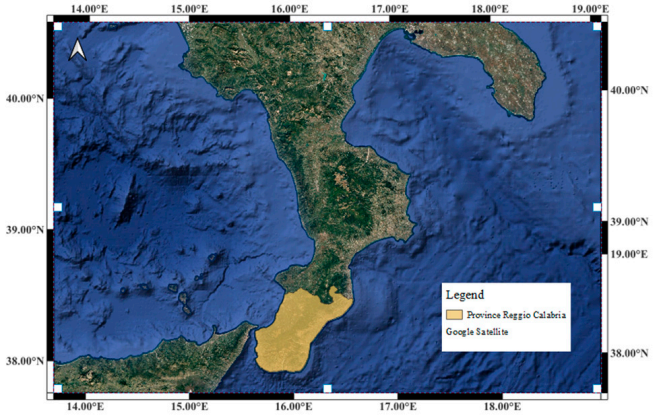


Figure 1. The selected study area: Province of Reggio Calabria, South Italy.

3. Methodology

The methodology presented in the following research work, aimed at identifying the correlations existing between climatic variables and water resources in the Calabrian territory, and the most suitable classification methods for the identification of areas at risk of drought, involved the use of different datasets, present in Google Earth Engine (GEE) [17], containing the main variables taken into consideration in this study: Land Surface Temperature (LST), Normalized Difference Vegetation Index (NDVI), Evapotranspiration (ETa), Global Precipitation Measurement (GPM), and the Normalized Difference Water Index (NDWI). These variables are part of the set of Essential Climate Variables (ECVs) defined by the GCOS (Global Climate Observing System) to which the Intergovernmental Panel on Climate Change (IPCC) refers in the sixth IPCC report (AR6) and which are fundamental for monitoring climate change [18].

To monitor and analyze the monotonic trend of climatic variables, the Mann–Kendall test [19], a non-parametric statistic known in the literature to identify growth or decrease

trends in time series, was applied to the variables and calculated according to the following analytical relationship (1).

$$s = \sum_{i-1}^{n-1} \sum_{j=i+1}^{n} sgn(x_j - x_i), \quad (1)$$

where the sgn function is defined as (2):

$$sgn(x_j - x_i) = \begin{cases} +1 \; se \; x_j - x_i > 0 \\ 0 \; se \; x_j - x_i = 0 \\ -1 \; se \; x_j - x_i < 0 \end{cases}, \quad (2)$$

and x represents the observed value of the variable under consideration (e.g., time series of monthly NDWI, precipitation, LST, etc.), x_i = observed value at time i.

The method was applied individually to the variables to identify specific behavioral trends. To avoid seasonal bias in trends, we applied the pre-whitening method, removing positive autocorrelation before applying the Mann–Kendall test. This allowed us to obtain more robust results without overestimating trends related to seasonal cyclicality. Moreover, the analysis was performed for the longest possible period present in GEE, as a longer series guarantees a more reliable test by reducing the risk of positive/negative phases due to the normal variability of climate data.

A key variable in characterizing the influence of climate change on water availability is LST, which is often obtained from meteorological stations scattered across the study area. In Calabria, particularly in the Municipality of Reggio Calabria, there is a network of stations capable of recording climate data daily. The limitation in using this dataset is the availability of discretely distributed, rather than continuous, data. It would therefore be necessary and indispensable to apply the correct spatial and temporal interpolation to the data recorded by the stations to obtain, with the least possible error, the behavior of climate variables at every point in the study area. For this reason, it was decided to use continuous data obtained from satellite observations. Temperature, in fact, is one of the parameters most studied and analyzed by satellite missions, especially in the last twenty years, and global datasets of both air and land surface temperature exist, with frequencies and resolutions that can be significantly different from each other. Compared to air temperature, land surface temperature can exhibit significant temperature variations, warming significantly during the day and cooling rapidly at night, depending on the soil's heat capacity. For the purposes of this work, it was decided to use air temperature, which is a factor that causes water evaporation and the lowering of water levels. Air temperature is present in CAMS (Copernicus Atmosphere Monitoring System) datasets [20], but at resolutions too high to perform local analysis. For this reason, air temperature was derived from Landsat 8 and 9 products [21,22]. To estimate Air Temperature (AT) data, the Temperature-Vegetation Index (TVX) method was used [23], which assumes that the greater the vegetation density, the lower the air temperature and vice versa, thus assuming a strongly negative correlation between LST and NDVI: as vegetation activity increases (high NDVI), LST tends to decrease [24]. The TVX method does not directly measure the air temperature but specifically was applied to estimate Air Temperature (AT) from LST and NDVI, which measure vegetation vigor, obtained from satellite data acquired by Sentinel-2 [25].

To make the analysis locally adaptable in time and space, a spatio-temporal moving window was used, within which a local linear regression between LST and NDVI is calculated, according to the following Equation (3):

$$\mathrm{LST}(i,j,t) = a(i,j,t)\cdot NDVI(i,j,t) + b(i,j,t) + \varepsilon(i,j,t), \quad (3)$$

where

- (i, j) are the spatial coordinates of the central pixel;
- t is the time;
- a and b are the regression coefficients estimated for each window;
- ε is the error term.

The moving window [26,27] was applied to a sequence of temporal data, subsampling the data and calculating the statistics (in this case, linear regression) for each window on that sample. We proceeded by moving the window for the entire dataset under consideration, by a specific temporal unit (t ± h), and for a predefined kernel (9 × 9).

So, for each point (i, j, t), the LST and NDVI values are extracted within the space-time window ($i \pm$ k, $j \pm$ k, $t \pm$ h), and the local regression is estimated. Once the coefficients a and b are obtained, the AT is estimated assuming that it corresponds to the LST in conditions of full vegetative cover (4):

$$AT(i,j,t) = a(i,j,t)\cdot NDVI_{max} + b(i,j,t) \quad (4)$$

where $NDVI_{max}$ represents the NDVI value in conditions of fully developed vegetation. As is known, NDVI was calculated using the following Equation (5):

$$NDVI = \frac{NIR - RED}{NIR + RED} \quad (5)$$

This approach allows for the more accurate identification and study of local trends that could be hidden during a global analysis, proving effective in the study of data with high spatial and temporal variability, such as in the case of climate variables. The end result of the process is a combination of multiple local regressions, producing a time series of AT estimates, where each point is the result of the calculated regression. The data considered in this work, as previously mentioned, were primarily analyzed and managed within the Google Earth Engine (GEE) cloud platform, which is a powerful cloud platform that allows data analysis and processing directly in the cloud.

As regards evaporation, it is the process by which surface moisture is transferred to the atmosphere and is a fundamental parameter for monitoring water availability in the region, allowing for a better understanding of the global water cycle. Its estimation has been difficult for years, but in the last 50 years, remote sensing has made a significant contribution and has allowed the estimation of this parameter to both global and regional scales. There are several models to determine the value of evapotranspiration, based on both temperature and conductance. Derardja et al. [28] provide a comprehensive review of the main temperature-based models for a more concise and precise evapotranspiration estimation, starting from the fundamental theories and moving on to the development, validation and the strengths and limitations of the various models.

Among the various products that provide estimated evapotranspiration, this research used the MODIS product [29], a sensor mounted on NASA's Terra and Aqua satellites. The MODIS-derived ET product is based on the modified Penman-Monteith model and calculates current evapotranspiration and potential evaporation from the Normalized Difference Vegetation Index (NDVI), Land Surface Temperature (LST), fraction of photosynthetically

active radiation absorbed (FAPAR), radiation, and meteorology. This product has a ground resolution of 500 m and a revisit time of 8 days.

For precipitation, the dataset from the international NASA and JAXA Global Precipitation Measurement (GPM) satellite mission was used [30], which provides global precipitation (rain and snow) data every 3 h. The instrument used, the TRMM (Tropical Rainfall Measuring Mission), allows calculation of precipitation intensity (mm/h), precipitation type, vertical distribution, frequency, and duration of events. It is therefore a comprehensive and useful dataset for ensuring global rainfall data.

The climate variables identified and analyzed in this work were then used to calculate the correlation with water resources. To analyze the quantity of water available annually, an approach was developed that allows calculation of this variable starting from an index extrapolated from remote sensing data, the NDWI, (6).

$$NDWI = \frac{GREEN - NIR}{GREEN + NIR}, \quad (6)$$

This index, as is known [31,32], monitors the presence of and variation in water and can be obtained from various optical satellite images, particularly from MODIS, Landsat, or Sentinel sensors. It is an index that varies from -1 to 1; positive values indicate the presence of water due to the fact that the latter absorbs a lot of energy in the infrared bands. Negative values, however, tend to reflect a lot of energy, and therefore negative values occur (such as dry soil, sand, and rocks). This index, in particular, was obtained from optical images of Sentinel-2 [33] (and therefore using the green and near-infrared bands). The results were also integrated with the results obtained from the Sentinel-1 radar satellite, using the following analytical Formula (7):

$$NDWI = \frac{(VH - VV)}{(VH + VV)}, \quad (7)$$

where

- VH: Vertically and horizontally polarized radar image (vertical–horizontal)
- VV: Vertically and vertically polarized radar image (vertical–vertical)

Sentinel-1 measures the reflection of microwaves from surfaces based on different polarization configurations. Sentinel-1, a synthetic aperture radar (SAR), uses different polarization modes: VV, VH, HH, and HV. Each of these polarizations interacts differently with land surfaces depending on their physical characteristics [34–37]. SAR data allows us to overcome calculation difficulties during cloudy or rainy seasons, as this signal can reach the land surface regardless of weather conditions [38,39].

Once the NDWI time series was obtained, the surface area attributable to the rivers was calculated, setting a threshold greater than 0.2 to identify areas presumably with the presence of water or wetlands. The water volume was then calculated using the DEM of the Province of Reggio Calabria and the Surface Volume function within the QGIS software (v. 3.40) [40].

Finally, the variables were analyzed using a Mann–Kendall test, and once all the necessary data had been collected, the spatio-temporal correlation analysis was performed using the Spearman test [41]. This test is a nonparametric test used to measure the strength and direction of a relationship between two variables. It is a nonparametric version of the Pearson test and is used in the literature when data are not normally distributed or when the relationship between the variables is nonlinear. The test was used to determine the

correlation between the dependent variable, and each of the climate variables considered, following Equation (8):

$$\rho = 1 - \frac{6 - \sum d_i^2}{n(n^2 - 1)}, \quad (8)$$

where

- d_i is the difference between the ranks of each pair of values ((X_i, Y_i) for the variable $\pm$ and the variable Y)
- n is the total number of data pairs (i.e., the sample size)

Once the correlations were determined and the dependence of each of the selected variables on water resources was determined, and after understanding the phenomena governing the water resource accumulation process, a dataset was created consisting of precipitation, temperature, and evapotranspiration data and indices calculated using Sentinel-2 satellite data.

The collected data served as a training dataset for classifying areas at risk of desertification. Specifically, these data were used to evaluate the performance of different classification models, allowing for a comparison of their effectiveness using the most common evaluation metrics, such as precision and accuracy. This comparative analysis enables the identification of the most suitable methods for effectively monitoring and managing desertification risks. In the study, we adopted a standard dataset split, with 80% training data and 20% testing data. To ensure the robustness of the models, we also implemented a 5-fold cross-validation.

Thanks to the exceptional capabilities of ensemble learning [42,43] in managing complex data with high precision, generalization, and robustness, we selected four popular artificial intelligence ensemble learning models for drought assessment: XGBoost [44], Random Forest (RF) [45], Logistic Regression (LR) [46], and Gradient Boosting Decision Trees (GBDT) [47].

Among these, GBDT effectively captures nonlinear relationships between assessment factors by combining the outputs of multiple decision trees, making it adept at handling complex, multi-source data. XGBoost enhances training and prediction efficiency through algorithmic optimizations and parallel processing, allowing it to excel with large datasets. Random Forest (RF) is particularly useful for evaluating the importance of various features, helping to identify key influencing factors while demonstrating resilience to overfitting. Logistic Regression (LR) is effective for analyzing and modeling potential linear relationships in susceptibility assessments to landslides.

The hyperparameters for each AI model were optimized using a grid search on a subset of the data. Specifically:

- Random Forest: 300 trees, max depth 10, min samples split 2.
- XGBoost: learning rate 0.1, max depth 8, 200 estimators, early stopping after 20 iterations.
- GBDT: learning rate 0.05, max depth 7, 150 estimators.
- Logistic Regression: solver 'lbfgs', C = 1.0.

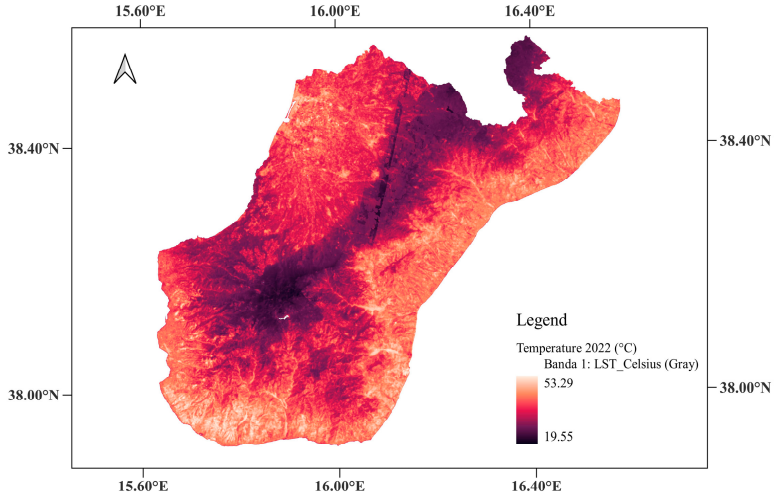
Finally, the main evaluation metrics of the classification methods were calculated.

The ROC curves were then determined [48], representing a curve in a graph where the True Positive Rate is plotted on the y-axis and the False Positive Rate on the x-axis.

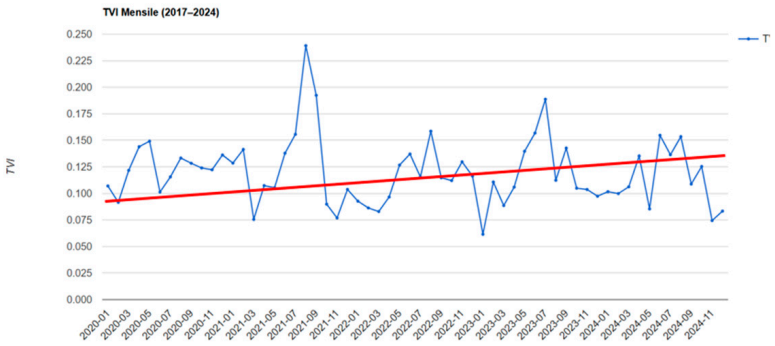
4. Results

The proposed methodology allowed us to evaluate the spatial as well as temporal trends of some climatic variables and therefore to be able to use them for the creation of a dataset useful for the classification of areas at risk of drought. Analyzing the time series of

AT data, it was possible to note a slight increase in this parameter over the years, confirming the global trend of temperature. An index from the TVX method was also calculated (TVI) to better understand the behavior of the variable. The results are shown in Figure 2a,b.



(**a**)



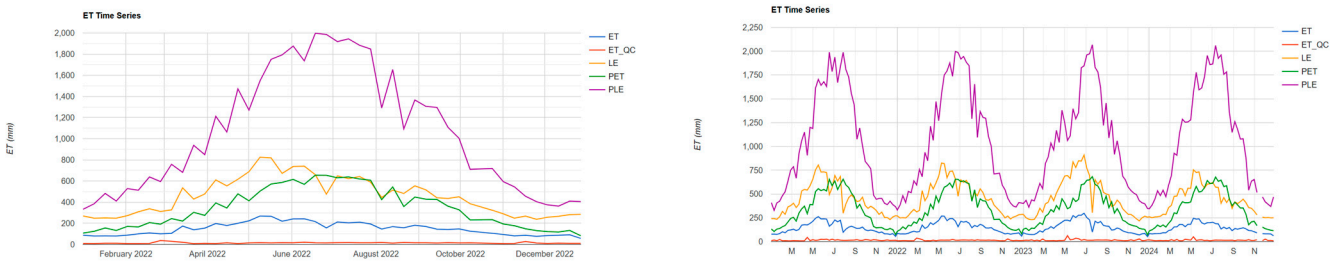
(**b**)

Figure 2. (**a**) Air Temperature 2022 (°C). Lighter colors represent higher temperatures exceeding 50 °C, while darker colors represent areas with temperatures around 20 °C. It is also important to highlight from these results the significant temperature range that occurs moving away from the coast.; (**b**) TVI trend from 2020 to 2024. The blue line represents the recorded values, while the red line shows the evidently growing trend.

The Mann–Kendall test showed a Z-score of +2.5, a *p*-value of 0.01, and a statistically significant "increasing" trend. These values suggest an increasing trend in estimated air temperature over the period considered.

Regarding evapotranspiration, the annual trend of this variable was studied. It increases significantly in the summer due to greater solar radiation, higher temperatures, stronger winds, and lower humidity. Higher temperatures, as recorded, contribute to greater soil evaporation, accelerating water passage and increasing plant transpiration. This also causes vegetative distress due to induced water stress and the altered hydrological cycle, which leads to a reduction in available soil water.

Figure 3a,b shows a graph highlighting the evapotranspiration time series for the province of Reggio Calabria and, Figure 4 the evapotranspiration map for the year 2022.



(**a**) (**b**)

Figure 3. (**a**) Evapotranspiration trend 2022; The various components of evapotranspiration and their monthly trend for the year 2022 are represented with different colors. As is evident from the graph, the highest values are reached in the summer period. (**b**) Evapotranspiration time series from 2021 to 2024. The various components of evapotranspiration and their yearly trend are represented with different colors.

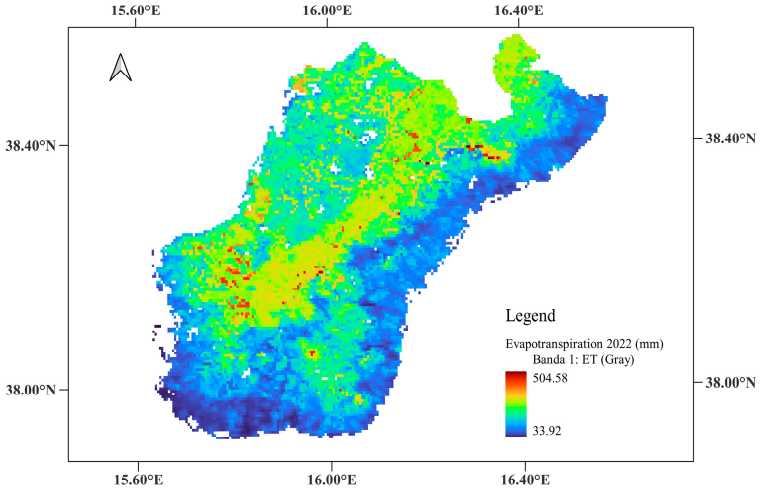


Figure 4. Evapotranspiration map 2022. The areas that are subject to a greater evapotranspiration phenomenon are shown in red, while the areas that are less subject to this phenomenon are shown in blue.

As regards precipitation, the analyzed time series highlighted a negative trend in precipitation, with a progressive decrease over time, showing how precipitation has become increasingly scarce. The Mann–Kendall test performed on this time series of precipitation showed a Z-score of −1.0 and a *p*-value of 0.20, with a decreasing trend, although the observed decrease could be attributable to natural precipitation variability rather than robust climate change over the period considered (Figure 5).

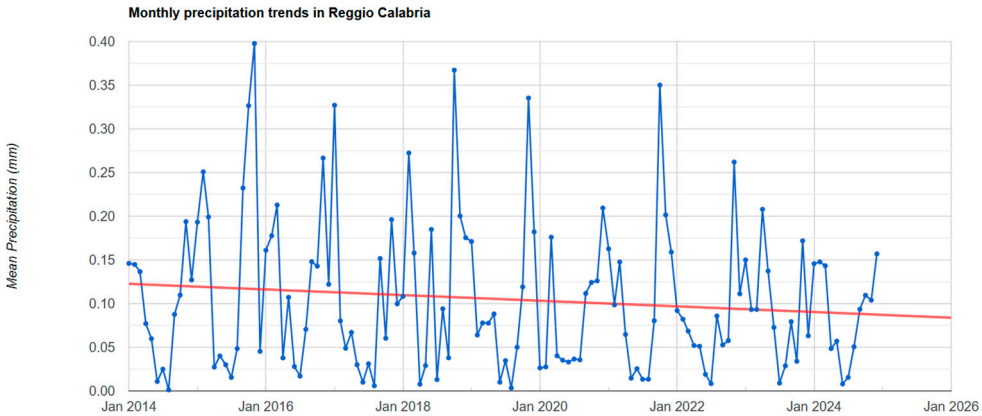


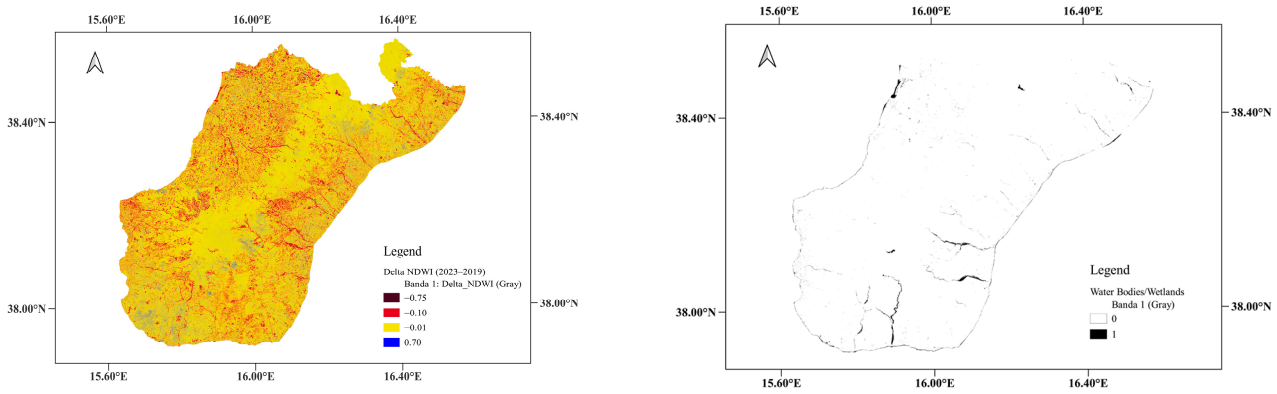
Figure 5. Precipitation trend from 2014 to 2024. The blue line represents the recorded values while the red line represents the overall annual trend.

As regards the volume of water, the trend of the NDWI for the study area was analyzed, obtaining important statistical evaluations summarized in Table 1.

Table 1. Main statistics for NDWI (2019–2023).

Statistics	Value
Delta_NDWI_max	0.878
Delta_NDWI_mean	−0.043
Delta_NDWI_min	−1.063
Delta_NDWI_stdDev	0.099
Area with increased NDWI	35,622,786.79 m^2
Area with decreased NDWI	45,738,557.51 m^2
% Increased NDWI	22.11%
% Decreased NDWI	77.88%

The time series used for the NDWI analysis runs from 2019 to 2023, considering only pixels with values above a threshold of 0.2. The results show an increase of 22.11% in some areas and a decrease, more marked near the rivers, of 77.88%. Figure 6a shows the delta of the NDWI between 2023 and 2019, highlighting in blue the areas that recorded an increase in the NDWI value, and therefore a positive delta indicating an increase in water content; in red, instead, the areas that experienced a decrease in the NDWI and therefore in water content. Finally, Figure 6b shows the NDWI extraction process that led to the determination of water volume using QGIS software.



(**a**) (**b**)

Figure 6. (**a**) NDWI difference 2023–2019; the areas that record a positive (blue) and negative (red/brown) difference in the NDWI value are shown. (**b**) Water bodies surface determined with NDWI data. The black color represents the areas where from the analyses carried out, water availability is evident, while the white color represents its absence. This result was used to determine water volume.

From the estimate made and the values reported in Table 1, a decrease in water resources of 34.17% was found. It should be emphasized that this is not the available volume in the water engineering sense (such as that stored in the dam), but a spatial-temporal estimate of the presence of surface water or water close to the surface, which includes rivers and seasonal water courses, reservoirs, temporary wetlands. The estimated uncertainty, based on a preliminary comparison with local reservoir volume data, is in the order of ±15%, which we consider acceptable for a territorial scale analysis.

Once the water content was obtained for the entire province through the process described above, the spatiotemporal correlation was calculated using the Spearman test between each of the climate variables and water volume.

For the Temperature-Water Volume correlation, the results revealed Spearman's rho coefficient of -0.682, indicating a strong and fairly marked negative correlation (Figure 7), and a low p-value ($p < 0.05$). Spearman's correlation between Evapotranspiration-Water Volume is equally negative, with a rho coefficient of -0.66 and a low p-value. With precipitation, this correlation becomes positive, with a rho of 0.30.

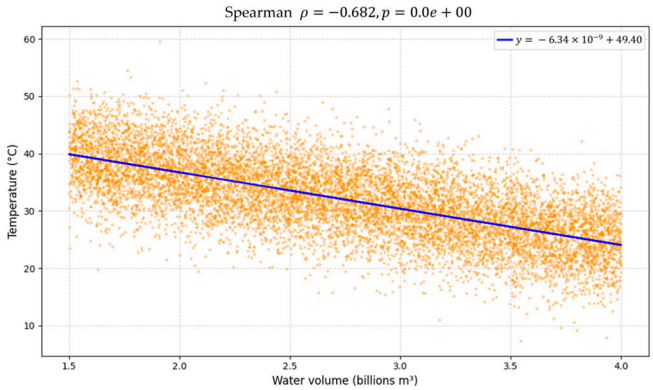


Figure 7. Scatterplot of the correlation between Temperature and Water Volume.

Finally, starting from these evaluations, as reported in the previous chapter, a dataset was created, and the different classification models were tested. In particular, the dataset was split into 80% training and 20% testing, applying stratified sampling to maintain the original class distribution. During the hyperparameter tuning phases and to estimate the variability of the performance metrics, a 5-fold stratified cross-validation was performed. The accuracy, precision, and AUC-ROC metrics were reported. The various models used showed very similar values, and all proved to be particularly effective in classifying areas at risk of drought. Below, a table (Table 2) summarizing the results obtained for the year 2023.

Table 2. Evaluation Metrics for AI classification methods.

Model	Precision	Accuracy
Random Forest	90%	93%
Logistic Regression	79%	85%
XGBoost	88%	91%
Gradient Boosting	85%	89%

From the results, it can be noted that the Random Forest model was one of the most effective, with a precision and accuracy of 90% and 93%, respectively. This is also evident from the ROC curve, which provides a more intuitive evaluation of the classifier's quality. Figure 8 shows the ROC curves, in which the red line represents the Random Forest model, the yellow line represents XGBoost, the green line represents Gradient Boosting, and the blue line represents Logistic Regression. An 80/20 split was applied to achieve class balance in the stratified sampling of the training and testing datasets, thereby preventing overestimation of True Negative (TN) values and ensuring a fair model evaluation. Additionally, to lessen bias and volatility in model performance, 5-fold cross-validation was used. Since the AUC-ROC metric offers a reliable assessment of discrimination ability and is independent of class distribution, it was employed as a complementary indicator.

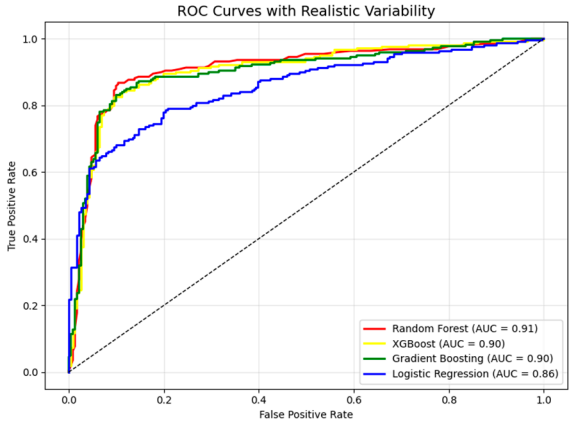
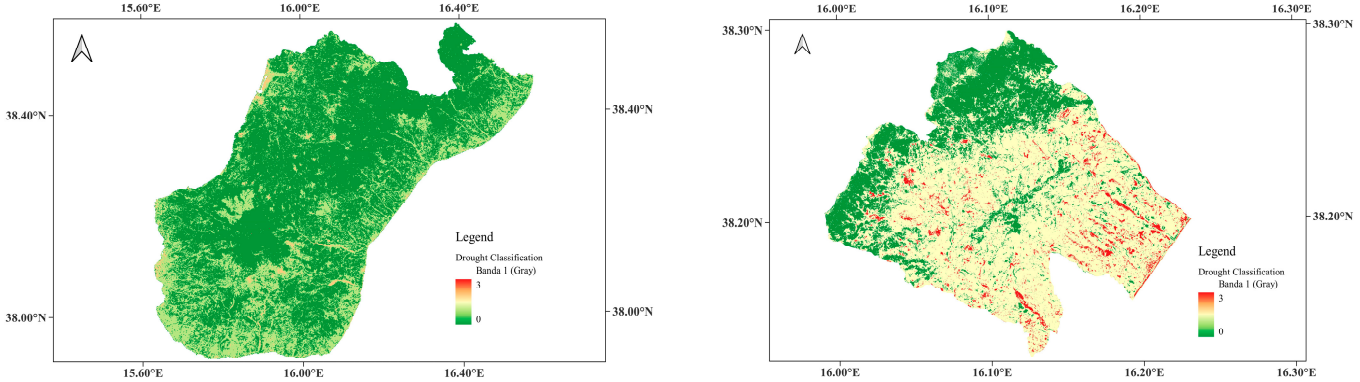


Figure 8. ROC curves for classification models: red line represents Random Forest, yellow line represents XGBoost, green line represents Gradient Boosting and blue line represents Logistic Regression.

In Figure 9a,b, the result of the Random Forest classifier is shown. Different colors represent areas of greater or lesser drought.



(**a**) (**b**)

Figure 9. (**a**) Drought Classification performed with Random Forest model for the entire Province of Reggio Calabria; (**b**) Drought Classification performed with Random Forest model for an area of the Aspromonte Geopark.

Finally, in Figure 10 the confusion matrix of the classification shown in Figure 9a,b is presented using the same model and obtaining the precision and accuracy shown in Table 2. The confusion matrix was computed for the Random Forest model using the test dataset (20% of total samples) after stratified 5-fold cross-validation. The matrix (Figure 10) reports normalized percentage values and was used to calculate precision, accuracy, and AUC-ROC metrics. The reliability of the model was confirmed by explicitly deriving the true positive (TP), true negative (TN), false positive (FP), and false negative (FN) rates from this matrix. It is important to specify that the Random Forest method is not exclusively valid for the study area, but can also be applied to other regions, following the same methodology. However, climate variables and their influence on water scarcity can vary significantly from one region to another, particularly in the presence of different climate conditions. In such cases, additional variables may come into play or broader considerations may be necessary. While the Random Forest method remains applicable, appropriate verification and testing with context-specific variables will be necessary to ensure the validity of the approach even in areas with different climatic characteristics.

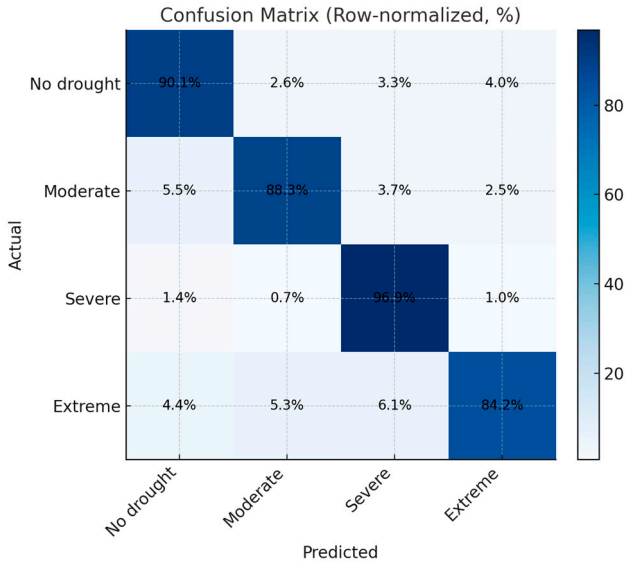


Figure 10. The confusion matrix of the classification obtained using the Random Forest classifier. The confusion matrix is row-normalized and presented with percentage values.

5. Discussion

The results obtained in this research first confirm the expected trends of increasing air temperature and decreasing precipitation, together with the consequent reduction in water availability. The analysis demonstrates that rising temperatures are directly associated with higher evapotranspiration rates, thereby intensifying plant water stress and enhancing soil moisture depletion. The Mann–Kendall test, applied to the multi-annual time series extracted via the Google Earth Engine (GEE) cloud-based platform, proved to be particularly effective in detecting the significance and direction of these trends. This confirms the importance of selecting temperature, precipitation, evapotranspiration, and vegetation indices as essential variables for drought monitoring. The availability of GEE allowed the processing of multi-temporal datasets without the need for local data storage, ensuring efficiency in both data management and analytical reproducibility.

Specifically, the study highlighted that evapotranspiration in 2022 reached anomalously high values in the Calabria region, coinciding with one of the most critical drought years in Italy. The NDWI-based analysis proved effective in quantifying the extent of surface water bodies, revealing a marked reduction in the water volumes stored in the main reservoirs. These findings were further supported by the correlation analysis between vegetation indices and climatic variables, which consistently pointed to vegetation greening responses under conditions of water deficit. Finally, the application of artificial intelligence methods demonstrated that ensemble classifiers—particularly Random Forest—achieved robust performance in identifying areas most exposed to desertification risk, offering a reliable basis for environmental monitoring and planning. When comparing these results with previous studies conducted in other Mediterranean areas or semi-arid regions, methodological differences become evident. In particular, while many studies rely on long-term reanalysis datasets at regional or continental scales, our work emphasized the integration of optical and SAR satellite data at a local scale, focusing on a region where hydro-climatic information is scarce. This enabled a more detailed characterization of reservoirs and smaller watercourses, which are often neglected in global products. Moreover, the use of GEE for trend analysis ensured methodological consistency, but the relatively short time span of available products (about five years for some indices) represents a limitation compared to the longer series typically used in global-scale drought assessments.

Furthermore, important hydrological feedback mechanisms can be used to analyze the observed relationships. Elevated air temperatures in Mediterranean ecosystems increase atmospheric evaporative demand, which raises potential evapotranspiration. This process increases vegetation water stress by decreasing plant transpiration efficiency and speeding up soil moisture loss. A positive feedback loop common in semi-arid environments, the decrease in canopy shading caused by declining plant cover intensifies local heating and evapotranspiration by increasing surface albedo and soil exposure. Strong negative correlations between temperature, evapotranspiration, and water availability in the study area are explained by these interactions, which offer a mechanistic insight that goes beyond statistical associations.

Despite the robustness of the approach, several uncertainties and limitations need to be acknowledged. First, the analysis was limited by the short temporal coverage of some datasets, which constrains the ability to capture long-term climatic oscillations. Second, the study only considered environmental drivers of drought, while anthropogenic factors—such as land use changes, water withdrawals, and agricultural intensification—were not explicitly included. Third, potential biases related to satellite acquisition conditions (e.g., cloud cover for optical sensors, speckle in SAR data) could affect the accuracy of the derived indices. Nevertheless, the methodological framework proposed here has important practical implications. The combination of satellite-derived indicators, non-parametric trend analysis, and machine learning classification provides local planners and decision-makers with timely and spatially detailed information for water resource management and drought risk mitigation. In particular, the results can support regional administrations in identifying priority areas for intervention, planning reservoir management strategies, and promoting more sustainable agricultural practices.

The study demonstrates the effectiveness of a cloud-based, remote-sensing-driven approach to monitoring water availability and drought dynamics on a local scale. By combining robust statistical methods with innovative classification algorithms, it offers a replicable methodology that can be extended to other regions with similar hydro-climatic challenges.

6. Conclusions

This study has demonstrated the potential of artificial intelligence models in analyzing climate variables and identifying drought-prone areas, with a specific focus on the Aspromonte National Park. The key findings demonstrate that (i) air temperature shows a statistically significant increasing trend ($Z = +2.5$, $p < 0.01$), while precipitation exhibits a decreasing tendency; (ii) water resources, estimated through NDWI, declined by approximately 34% between 2019 and 2023; (iii) temperature and evapotranspiration are strongly and negatively correlated with water availability ($\rho = -0.68$ and -0.66, respectively); and (iv) the Random Forest model achieved the highest classification accuracy (93%) in mapping drought-prone areas. These findings confirm the reliability of combining non-parametric trend analysis and AI classification for local-scale drought monitoring and constitute the principal scientific contribution of the work. The results obtained highlight the importance of combining multivariate climate data with advanced AI techniques to support data-driven decision-making processes in environmental management and territorial planning. Beyond identifying the most effective predictive model, this research provides a methodological framework that is replicable and adaptable to other regions facing similar challenges. The integration of geospatial data with machine learning techniques not only enhances the understanding of climate dynamics but also offers a powerful tool for proactive planning and climate adaptation strategies.

The approach used can also be extended by analyzing the role of AI in supporting spatial planning through the implementation of nature-based solutions and urban regeneration

policies. By correlating climatic variables with urban planning indicators, stakeholders can better assess vulnerabilities and design targeted interventions that are both sustainable and resilient. Moreover, the potential for multitemporal analyses offers a valuable opportunity to quantify the historical impact of climate change on ecosystems and human settlements. This retrospective capability could be further enhanced through the integration of remote sensing data and high-resolution environmental monitoring systems.

Future developments of this research may include the expansion of the model to incorporate socio-economic indicators, enhancing its utility for holistic climate risk assessments; the application of the model to simulate future climate scenarios under different emission pathways (e.g., RCP or SSP scenarios); the development of a decision-support system accessible to local authorities, planners, and conservation agencies for real-time monitoring and response; and the extension of the temporal coverage of the datasets employed, the integration of in situ hydrological and meteorological observations for validation, and inclusion of socio-economic indicators and land use dynamics to provide a more comprehensive view of drought risk. Moreover, the adoption of advanced artificial intelligence techniques, such as deep learning and convolutional neural networks applied to geospatial data, could further improve classification performance, although at the cost of higher computational demands.

For this reason, the proposed approach represents a promising direction in the use of remote sensing and artificial intelligence for environmental sustainability. Their combined application can significantly contribute to improving climate resilience, particularly in ecologically sensitive and biodiversity-rich areas such as Aspromonte, by fostering a more informed, anticipatory, and adaptive territorial governance.

Author Contributions: Conceptualization, E.G., C.M. and V.B.; methodology, E.G., C.M. and V.B.; software, E.G., C.M. and V.B.; validation, E.G., C.M. and V.B.; formal analysis, E.G., C.M. and V.B.; investigation, E.G., C.M. and V.B.; resources, E.G., C.M. and V.B.; data curation, E.G., C.M. and V.B.; writing—original draft preparation, E.G., C.M. and V.B.; writing—review & editing, E.G., C.M. and V.B.; visualization, E.G., C.M. and V.B.; supervision, E.G., C.M. and V.B.; project administration, E.G., C.M. and V.B.; funding acquisition, E.G., C.M. and V.B. All authors have read and agreed to the published version of the manuscript.

Funding: This research received no external funding.

Institutional Review Board Statement: Not applicable.

Informed Consent Statement: Not applicable.

Data Availability Statement: The data presented in this study are derived from publicly available datasets. Specifically, this research contains Copernicus Sentinel-1 and Sentinel-2 data (2025), MODIS data (NASA LP DAAC, 2025), and Global Monthly Precipitation data (NASA GPM, 2025). These datasets were processed and modified by the authors for analysis in this study.

Conflicts of Interest: The authors declare no conflicts of interest.

References

1. Blauhut, V.; Stahl, K.; Stagge, J.H.; Tallaksen, L.M.; De Stefano, L.; Vogt, J. Estimating drought risk across Europe from reported drought impacts, drought indices, and vulnerability factors. *Hydrol. Earth Syst. Sci.* **2016**, *20*, 2779–2800. [CrossRef]
2. EcoAtlante. Available online: https://sinacloud.isprambiente.it/portal/apps/storymaps/stories/7dccdae135854c99890ad09309f229fb (accessed on 16 June 2025).
3. Colglazier, W. Sustainable development agenda: 2030. *Science* **2015**, *349*, 1048–1050. [CrossRef] [PubMed]
4. Wang, X.; Xie, H. A review on applications of remote sensing and geographic information systems (GIS) in water resources and flood risk management. *Water* **2018**, *10*, 608. [CrossRef]

5. Hussain, M.F.; Meng, X.; Shah, S.F.; Hussain, M.A. Integrating spatiotem-poral analysis of land transformation and urban growth in Peshawar Valley and its implications on temperature in response to climate change. *ISPRS Int. J. Geo-Inf.* **2024**, *13*, 239. [CrossRef]
6. Weiss, F.; von Wehrden, H.; Linde, A. Long-term drought triggers severe de-clines in carabid beetles in a temperate forest. *Ecography* **2024**, *2024*, e07020. [CrossRef]
7. Němec, J.; Schaake, J. Sensitivity of water resource systems to climate variation. *Hydrol. Sci. J.* **1982**, *27*, 327–343. [CrossRef]
8. Xu, Z.X.; Chen, Y.N.; Li, J.Y. Impact of climate change on water resources in the Ta-rim River basin. *Water Resour. Manag.* **2004**, *18*, 439–458. [CrossRef]
9. Moses, O.; Hambira, W.L. Effects of climate change on evapotranspiration over the Okavango Delta water resources. *Phys. Chem. Earth* **2018**, *105*, 98–103. [CrossRef]
10. Yang, Y.; Roderick, M.L.; Guo, H.; Miralles, D.G.; Zhang, L.; Fatichi, S.; Luo, X.; Zhang, Y.; McVicar, T.R.; Tu, Z.; et al. Evapotranspiration on a greening Earth. *Nat. Rev. Earth Environ.* **2023**, *4*, 626–641. [CrossRef]
11. Barrile, V.; Genovese, E. GIS-Like environments and HBIM integration for ancient villages management and dissemination. *Int. Arch. Photogramm. Remote Sens. Spat. Inf. Sci.* **2024**, *48*, 41–47. [CrossRef]
12. Bilotta, G.; Meduri, G.M.; Genovese, E.; Bibbò, L.; Barrile, V. Safeguarding the Aspromonte Forests: Random Forests and Markov Chains as Forecasting Models for Predicting Land Transformations. *Forests* **2025**, *16*, 290. [CrossRef]
13. Bilotta, G.; Bibbò, L.; Meduri, G.M.; Genovese, E.; Barrile, V. Deep Learning Innovations: ResNet Applied to SAR and Sentinel-2 Imagery. *Remote Sens.* **2025**, *17*, 1961. [CrossRef]
14. Tripathi, S.; Trigunait, R. Achieving sustainable practices: Environmental sustainability and semi-supervised learning for carbon footprint reduction. *Environ. Dev. Sustain.* **2024**, 1–28. [CrossRef]
15. Essamlali, I.; Nhaila, H.; El Khaili, M. Supervised machine learning approaches for predicting key pollutants and for the sustainable enhancement of urban air quality: A systematic review. *Sustainability* **2024**, *16*, 976. [CrossRef]
16. Lima, R.P.; Silva, D.D.; Moreira, M.C.; Passos, J.B.; Coelho, C.D.; Elesbon, A.A. Development of an annual drought classification system based on drought severity indexes. *An. Acad. Bras. Ciências* **2019**, *91*, e20180188. [CrossRef] [PubMed]
17. Zhao, Q.; Yu, L.; Li, X.; Peng, D.; Zhang, Y.; Gong, P. Progress and trends in the application of Google Earth and Google Earth Engine. *Remote Sens.* **2021**, *13*, 3778. [CrossRef]
18. IPCC. Summary for Policymakers. In *Climate Change 2023: Synthesis Report*; Contribution of Working Groups I, II and III to the Sixth Assessment Report of the Intergovernmental Panel on Climate Change; Core Writing Team, Lee, H., Romero, J., Eds.; IPCC: Geneva, Switzerland, 2023; pp. 1–34. [CrossRef]
19. McLeod, A.I. Kendall rank correlation and Mann-Kendall trend test. *R Package Kendall* **2005**, *602*, 1–10.
20. Schroedter-Homscheidt, M.; Arola, A.; Killius, N.; Lefèvre, M.; Saboret, L.; Wandji, W.; Wald, L.; Wey, E. The Copernicus atmosphere monitoring service (CAMS) radiation service in a nutshell. In Proceedings of the 22nd SolarPACES Conference 2016, Abu Dhabi, United Arab Emirates, 11–14 October 2016.
21. Acharya, T.D.; Yang, I. Exploring landsat 8. *Int. J. IT Eng. Appl. Sci. Res. (IJIEASR)* **2015**, *4*, 4–10.
22. Markham, B.L.; Jenstrom, D.; Masek, J.G.; Dabney, P.; Pedelty, J.A.; Barsi, J.A.; Montanaro, M. Landsat 9: Status and plans. In *Earth Observing Systems XXI*; SPIE: Bellingham, WA, USA, 2016; Volume 9972, pp. 127–132.
23. Higuchi, A.; Hiyama, T.; Fukuta, Y.; Suzuki, R.; Fukushima, Y. The behaviour of a surface temperature/vegetation index (TVX) matrix derived from 10-day composite AVHRR images over monsoon Asia. *Hydrol. Process. Int. J.* **2007**, *21*, 1157–1166. [CrossRef]
24. Marzban, F.; Sodoudi, S.; Preusker, R. The influence of land-cover type on the relationship between NDVI–LST and LST-T air. *Int. J. Remote Sens.* **2018**, *39*, 1377–1398. [CrossRef]
25. Phiri, D.; Simwanda, M.; Salekin, S.; Nyirenda, V.R.; Murayama, Y.; Ranagalage, M. Sentinel-2 data for land cover/use mapping: A review. *Remote Sens.* **2020**, *12*, 2291. [CrossRef]
26. Shin, N.H.; Lee, S.H.; Kim, C.S. Moving window regression: A novel approach to ordinal regression. In Proceedings of the IEEE/CVF Conference on Computer Vision and Pattern Recognition, New Orleans, LA, USA, 18–24 June 2022; pp. 18760–18769.
27. Markham, K.; Frazier, A.E.; Singh, K.K.; Madden, M. A review of methods for scaling remotely sensed data for spatial pattern analysis. *Landsc. Ecol.* **2023**, *38*, 619–635. [CrossRef]
28. Derardja, B.; Kha-dra, R.; Abdelmoneim, A.A.A.; El-Shirbeny, M.A.; Valsamidis, T.; De Pasquale, V.; Deflorio, A.M.; Volden, E. Advancements in remote sensing for evapotranspiration estimation: A comprehensive review of temperature-based models. *Remote Sens.* **2024**, *16*, 1927. [CrossRef]
29. Savtchenko, A.; Ouzounov, D.; Ahmad, S.; Acker, J.; Leptoukh, G.; Koziana, J.; Nickless, D. Terra and Aqua MODIS products available from NASA GES DAAC. *Adv. Space Res.* **2004**, *34*, 710–714. [CrossRef]
30. Smith, E.A.; Asrar, G.; Furuhama, Y.; Ginati, A.; Mugnai, A.; Nakamura, K.; Adler, R.F.; Chou, M.-D.; Desbois, M.; Durning, J.F.; et al. International global precipitation measurement (GPM) program and mission: An overview. In *Measuring Precipitation from Space: EURAINSAT and the Future*; Springer: Dordrecht, The Netherlands, 2007; pp. 611–653.

31. Özelkan, E. Water body detection analysis using NDWI indices derived from landsat-8 OLI. *Pol. J. Environ. Stud.* **2020**, *29*, 1759–1769. [CrossRef] [PubMed]
32. Singh, K.V.; Setia, R.; Sahoo, S.; Prasad, A.; Pateriya, B. Evaluation of NDWI and MNDWI for assessment of waterlogging by integrating digital elevation model and groundwater level. *Geocarto Int.* **2015**, *30*, 650–661. [CrossRef]
33. Yang, X.; Zhao, S.; Qin, X.; Zhao, N.; Liang, L. Mapping of urban surface water bodies from Sentinel-2 MSI imagery at 10 m resolution via NDWI-based image sharpening. *Remote Sens.* **2017**, *9*, 596. [CrossRef]
34. Greifeneder, F.; Notarnicola, C.; Hahn, S.; Vreugdenhil, M.; Reimer, C.; Santi, E.; Paloscia, S.; Wagner, W. The added value of the VH/VV polarization-ratio for global soil moisture estimations from scatterometer data. *IEEE J. Sel. Top. Appl. Earth Obs. Remote Sens.* **2018**, *11*, 3668–3679. [CrossRef]
35. Li, J.; Wang, S. Using SAR-derived vegetation descriptors in a water cloud model to improve soil moisture retrieval. *Remote Sens.* **2018**, *10*, 1370. [CrossRef]
36. Ullmann, T.; Schmitt, A.; Jagdhuber, T. Two component decomposition of dual polarimetric HH/VV SAR data: Case study for the tundra environment of the Mackenzie Delta region, Canada. *Remote Sens.* **2016**, *8*, 1027. [CrossRef]
37. Bhogapurapu, N.; Mandal, D.; Rao, Y.S.; Bhattacharya, A. Soil moisture retrieval using SAR derived vegetation descriptors in water cloud model. In Proceedings of the IGARSS 2020-2020 IEEE International Geoscience and Remote Sensing Symposium, Waikoloa, HI, USA, 26 September–2 October 2020; pp. 4696–4699.
38. Thies, B.; Bendix, J. Satellite based remote sensing of weather and climate: Recent achievements and future perspectives. *Meteorol. Appl.* **2011**, *18*, 262–295. [CrossRef]
39. Ling, J.; Zhang, H.; Lin, Y. Improving urban land cover classification in cloud-prone areas with polarimetric SAR images. *Remote Sens.* **2021**, *13*, 4708. [CrossRef]
40. Khan, S.; Mohiuddin, K. Evaluating the parameters of ArcGIS and QGIS for GIS Applications. *Int. J. Adv. Res. Sci. Eng.* **2018**, *7*, 582–594.
41. Bishara, A.J.; Hittner, J.B. Testing the significance of a correlation with nonnormal data: Comparison of Pearson, Spearman, transformation, and resampling approaches. *Psychol. Methods* **2012**, *17*, 399. [CrossRef]
42. Dong, X.; Yu, Z.; Cao, W.; Shi, Y.; Ma, Q. A survey on ensemble learning. *Front. Comput. Sci.* **2020**, *14*, 241–258. [CrossRef]
43. Polikar, R. Ensemble learning. In *Ensemble Machine Learning*; Springer: New York, NY, USA, 2012; pp. 1–34.
44. Zhen, J.; Mao, D.; Shen, Z.; Zhao, D.; Xu, Y.; Wang, J.; Jia, M.; Wang, Z.; Ren, C. Performance of xgboost ensemble learning algorithm for mangrove species classification with multisource spaceborne remote sensing data. *J. Remote Sens.* **2024**, *4*, 0146. [CrossRef]
45. Barrile, V.; Bibbò, L.; Bilotta, G.; Meduri, G.M.; Genovese, E. Geomatics Innovation and Simulation for Landslide Risk Management: The Use of Cellular Automata and Random Forest Automation. *Appl. Sci.* **2024**, *14*, 11853. [CrossRef]
46. Khurshid, H.; Khan, M.F. Segmentation and classification using logistic regression in remote sensing imagery. *IEEE J. Sel. Top. Appl. Earth Obs. Remote Sens.* **2014**, *8*, 224–232. [CrossRef]
47. Ghatkar, J.G.; Singh, R.K.; Shanmugam, P. Classification of algal bloom species from remote sensing data using an extreme gradient boosted decision tree model. *Int. J. Remote Sens.* **2019**, *40*, 9412–9438. [CrossRef]
48. Baker, S.G. The central role of receiver operating characteristic (ROC) curves in evaluating tests for the early detection of cancer. *J. Natl. Cancer Inst.* **2003**, *95*, 511–515. [CrossRef]

Disclaimer/Publisher's Note: The statements, opinions and data contained in all publications are solely those of the individual author(s) and contributor(s) and not of MDPI and/or the editor(s). MDPI and/or the editor(s) disclaim responsibility for any injury to people or property resulting from any ideas, methods, instructions or products referred to in the content.